Nonlinear Seismic Response of Concentrically Braced Frames using Finite Element Models

J.P. English & J. Goggins
College of Engineering and Informatics, National University of Ireland, Galway, Ireland

15 WCEE
LISBOA 2012

SUMMARY

This paper investigates the accuracy of three dimensional finite element models (FEMs) in predicting the response of dissipating members in a concentrically braced frame (CBF) under cyclic actions. The brace together with its connecting gusset plate are the main focus of this study. While it is acknowledged that the brace is the primary dissipating member of a CBF, the inelastic behaviour of the gusset plate as a second source of energy dissipation is of particular significance. A number of gusset-brace configurations were modelled with varying geometries and slenderness and verified against physical pseudo-static component and member tests. Recommendations are then made for modelling and designing end connections of brace members containing beam-column connections.

Keywords: Finite element modelling, gusset plates, concentrically braced frames, cyclic loading.

1. INTRODUCTION

Concentrically braced frames (CBFs) are an economic means of resisting lateral demands induced from earthquakes. This lateral resistance is predominately associated with the brace member, although a certain amount will inevitably come from the beam-column connection and the gusset plate. For simple CBFs, it is standard practice to ignore any lateral resistance from the connection of the brace member to the beam and column. In other words, the beam-column connections, as shown for example in Figure 1.1, are assumed to be pinned, when in fact the presence of the gusset plate can add significant lateral stiffness to the joint. The actual stiffness of the frame is complex in nature due to the behaviour of the gusset-brace system. When the brace member is subject to tension demands, the gusset plate will experience an added compressive stress in conjunction with the tensile stresses induced by the brace. This compressive stress is associated with the rotation of the beam-column joint as the CBF drifts laterally. The extent of this rotation is dependent on the amount of lateral drift and also the dimensions of the frame.

The overall stiffness of the CBF is thus a combination of that provided by the brace member and gusset plate connection to both brace and beam-column. This total stiffness will vary significantly depending on the relevant level of frame drift. At low cyclic demands the stiffness of the CBF will have similar contributions from both the tension and compressive gusset-brace system. As these cyclic demands increase and the brace and/or gusset plate experience buckling from compression loading, the lateral stiffness of the frame will become predominantly dependent on the tension resistance of the gusset-brace system only. These observations were also made by Goggins *et al.* (2005) for cyclic tests on brace members only. Currently, standard practice in Europe (CEN 2004) is that CBFs are designed so that yielding of the diagonals in tension will take place before failure of the connections and before yielding or buckling of the beams or columns. In the analysis of the structure, in frames with diagonal bracings only the tension diagonals are taken into account, while in frames with V bracings, both the tension and compression diagonals are taken into account for the seismic action. If a non-linear static (pushover) global analysis or non-linear time history analysis is used and certain criteria are met, both

tension and compression diagonals can be taken into account in the analysis of any type of concentric bracing system.

This current study, through experimental and numerical models, investigates if the contribution of the gusset plate to the lateral stiffness and energy dissipation of the system is significant. The main parameters of this system under consideration include the brace and gusset geometries (which include for cross section capacities and slenderness) and the level of connectivity between both members of the system and to the beam-column (see Figure 1.1). The effects of monotonic and cyclic loading are used to develop improved design procedures for gusset plates including the combined gusset-brace system. Monotonic simulations are used to develop a system to calculate the effective properties of the gusset plate and hence their tensile and compressive capacities. This method adopts an affective area approach based on an elliptical failure mode throughout the plate, similar to the $8t_p$ method proposed by Lehman et al. (2008), but with a modification factor to take account of the observed effective area utilised in the plates in this study. Cyclic simulations are then used to determine the ductility and energy dissipation of the combined gusset-brace system and comparisons are made to an equivalent brace-only system. To date, several test schemes and numerical FE models have been completed to simulate the behaviour of the brace member and the full CBF subject to cyclic loading (Goggins 2004; Goggins et al. 2005; Yoo et al. 2009; Nip et al. 2010a; Nascimbene et al. 2012; Stoakes and Fahnestock 2012). However, to the authors' knowledge a thorough study of the interactions of the gusset-brace system, including their relative stiffness, slenderness and axial capacities have yet to be fully explored.
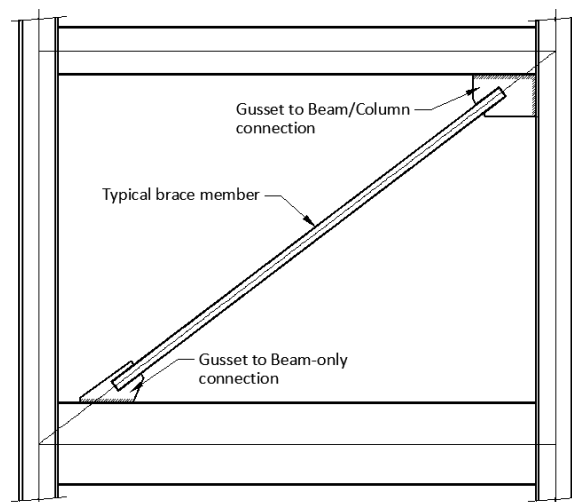
Figure 1.1. Typical CBF showing both a beam-column and a beam-only gusset connection.

2. EXPERIMETAL TEST SET-UP AND RESULTS

A series of experimental tests were conducted on gusset plates to obtain a thorough understanding of the failure modes and critical fracture locations. These were component tests on the plates and ignored the affects of the brace member and full frame actions; although effort was made to include rotations into a selected number of specimens to approximately simulate frame rotations combined with axial load from the brace, as shown in Figure 2.1.

As these component tests did not include a full length brace member, verification of the brace behaviour in the numerical models was made through existing experimental data obtained from Goggins (2004) and Nip et al. (2010a; 2010b). Both of these test series fully explored the cyclic behaviour of several different brace sections and normalised slenderness. However, only the work carried out by Nip et al. (2010a; 2010b) included an in-depth study of the cyclic material properties of the brace specimen subject to extremely low cycle fatigue tests.
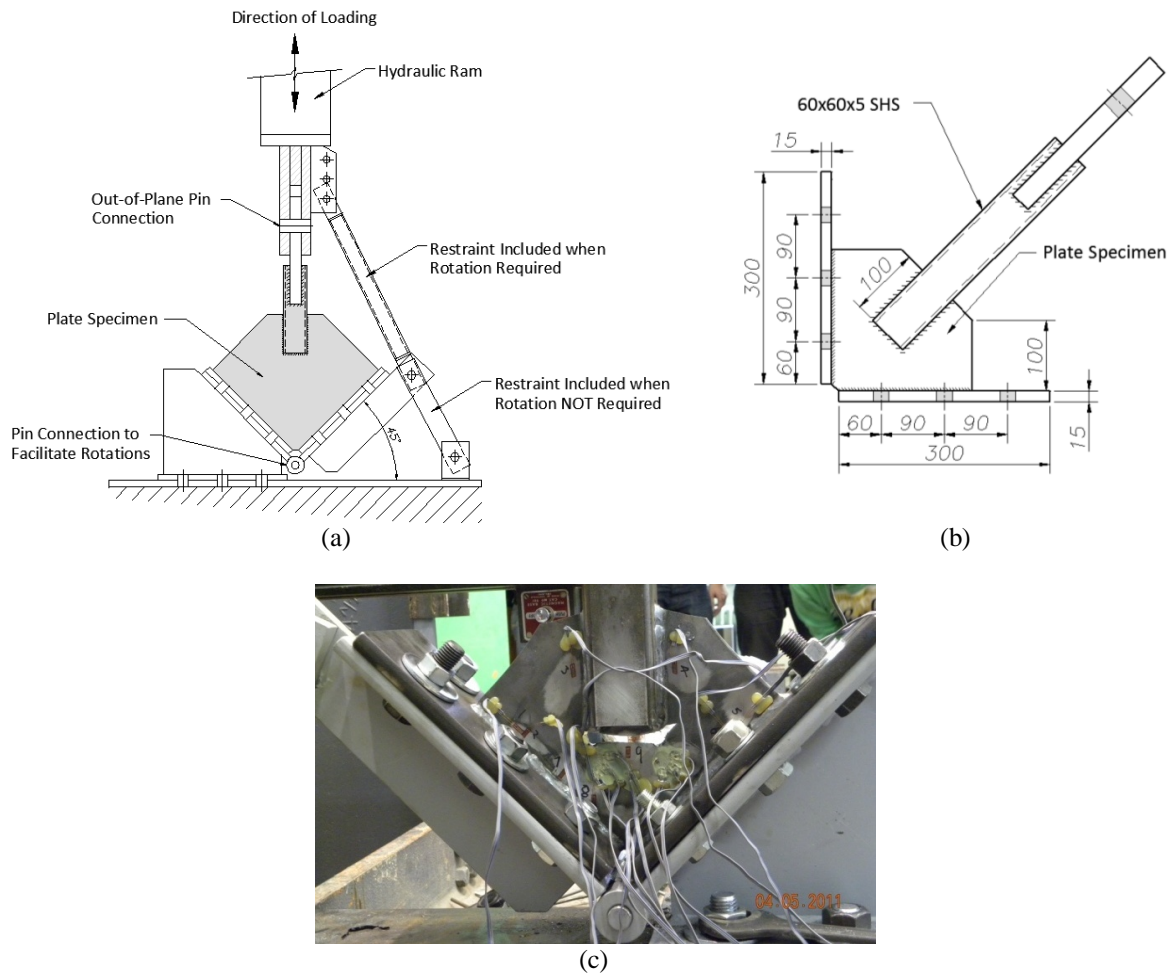
Figure 2.1.(a)-(c): (a) Test setup of specimen showing position of pin to allow plate rotations, (b) details of gusset plate specimen SP3a and (c) specimen SP3a after fracture.

3. NUMERICAL MODEL

In order to study the behaviour and performance of the gusset-brace system thoroughly, three systems were modelled: (1) Gusset plate only similar to the experimental set-up shown in Figure 2.1, (2) Brace element only, similar to the experimental set-up by Goggins (2004) and Nip *et al.* (2010), (3) gusset-brace assembly that represent details employed in buildings. The first two sets of models were to validate the numerical model, while the third set was used to carry out a parametric study on realistic systems employed in buildings. The finite element package ABAQUS (2009) was used to carry out the numerical analyses using three-dimensional finite element (FE) models. A four-node doubly curved general-purpose shell element (S4R) was utilised for both the brace member and gusset plate. This type of shell element has successfully been used to conduct similar such studies on brace members, gusset plates and CBFs (Goggins 2004; Goggins *et al.* 2005; Yoo *et al.* 2009; Nip *et al.* 2010a; Nascimbene *et al.* 2012; Stoakes and Fahnestock 2012). Mesh refinements were required in the gusset plate and the brace member in locations where local buckling and fracture were anticipated. From experimental observations made during the gusset components tests described in Section 2, fracture occurred in the plate at the end of the brace member and hence the refined mesh in this region. Local buckling and subsequently fracture occurred in the brace member at mid-span and also near the brace end. Local buckling at the brace end only occurs when the end connection is rigid or substantially rigid, which occurs when the gusset plates are relatively thick and stocky compared to the brace. For the most part, no local buckling was observed in the brace end when connected to a gusset plate designed by the $8t_p$ method (prescribed by Lehman *et al* 2008).

In the brace-only model and brace-gusset assembly, global buckling was accounted for in the models by inducing an imperfection in the form of a lateral displacement at mid-span of the brace member. This lateral imperfection was chosen as L/1000, where L is the length of the equivalent brace-only model. For the calibration simulations, L is simply the full length of the actual brace. To carry out the cyclic analysis, a bilinear plastic material model with kinematic hardening was used which allows for the Baushinger effect associated with cyclic loading. The numerical model can capture the salient response features of the physical experiments carried out by Goggins (2004) and Nip *et al.* (2010a; 2010b) on the brace-only member (see, for example, Figure 3.1). On the other hand, the model more closely mimicked the response of the tests conducted by Nip *et al.* (2010a; 2010b), as more detailed plastic material properties existed for these specimens. These specimens were hot-rolled hollow structural steel, whereas tests by Goggins (2004) were on cold-formed hollow structural steel members. As validation of the model was completed to several different test programmes, the material properties of each were used accordingly. For the parametric study discussed in Section 4, an average of the material properties obtained by Nip *et al.* (2010a) for the hot rolled steel tubular sections was adopted and implemented into the FE model using a tangent modulus of 1% of the Young's Modulus. The numerical study was conducted on the gusset-brace system under displacement controlled symmetric cyclic loading. As the gusset plate and brace can buckle and due to the unsymmetrical nature of the gusset plates, only one line of symmetry could be utilised at mid-span of the brace member, as seen in Figure 3.2.
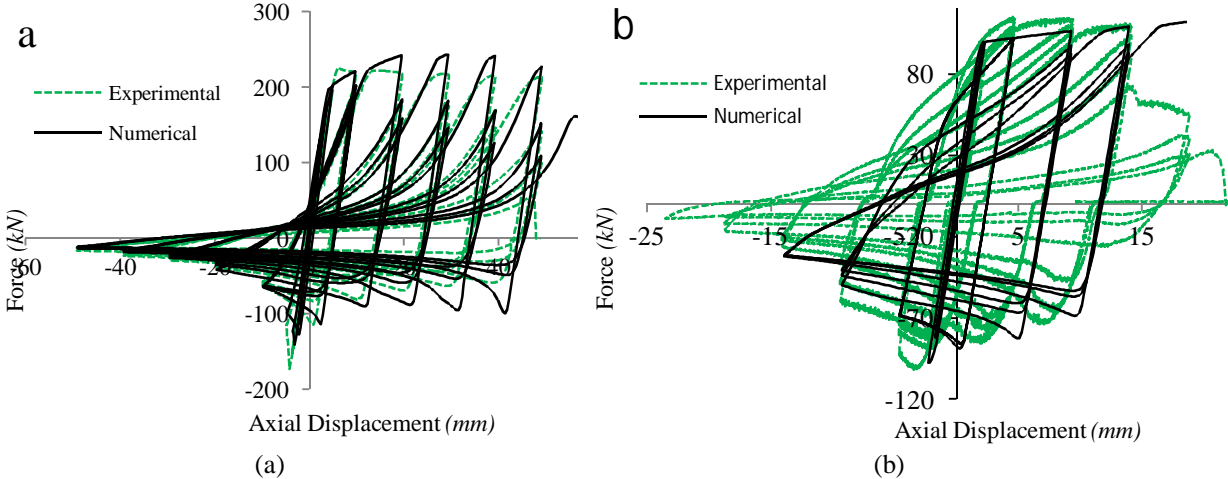
Figure 3.1. (a)-(b): Experimental hysteretic brace response of (a) 40x40x3x2050-CS-HR-Nip and (b) 40x40x2.5x1100-CS-CF-Goggins.
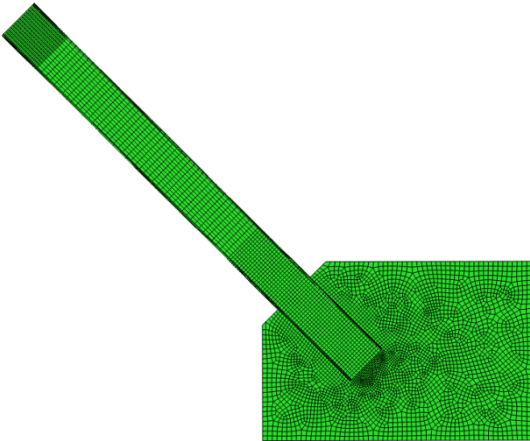
Figure 3.2. Model of half of Specimen GP05-10-S1S

4. PARAMETRIC STUDY

A parametric study is being conducted to explore the various differences inherent in gusset-brace connections commonly found in CBFs. This includes the relative capacities (in both tension and compression) of the gusset plate and connecting hollow brace section, the difference in normalised slenderness, $\bar{\lambda}$, effective gusset plate areas, A_E, and type of gusset plate connection (i.e. to beam and column or beam only – See Figure 1.1). The ductility and energy dissipation of the gusset-brace system is also compared to that of an equivalent brace-only system typically used when calculating CBF properties. To capture these parameters, this parametric study has been broken into three separate loading studies – monotonic, pseudo-static cyclic and real-time earthquake records. Preliminary findings from the first two loading studies on gusset-only and gusset-brace systems will be presented here. This parametric study will be validated using real-time full-scale shake table tests on single storey concentrically braced frames, which will be carried out in Autumn 2012 as part of the EU-FP7 TNA SERIES project 'BRACED' (Broderick *et al.* 2011).

The numerical model described in Section 3 has been employed in the parametric study. Firstly, a monotonic study is used to capture an improved understanding of the plate behaviour and develop an accurate procedure for calculating the effective area of the gusset plates for the prediction of their tensile and compressive capacities. Secondly, the cyclic study is performed to capture the ductility and energy dissipation of the brace-gusset system under pseudo-static load conditions.

The study sampling has numerous variables including brace cross section and slenderness, gusset geometries (shape and thickness – see Figure 4.1), brace angle, brace connection length L_c and gusset connectivity. The gusset connectivity includes connection to both beam and column or alternatively to the beam only, as shown in Figure 4.1.
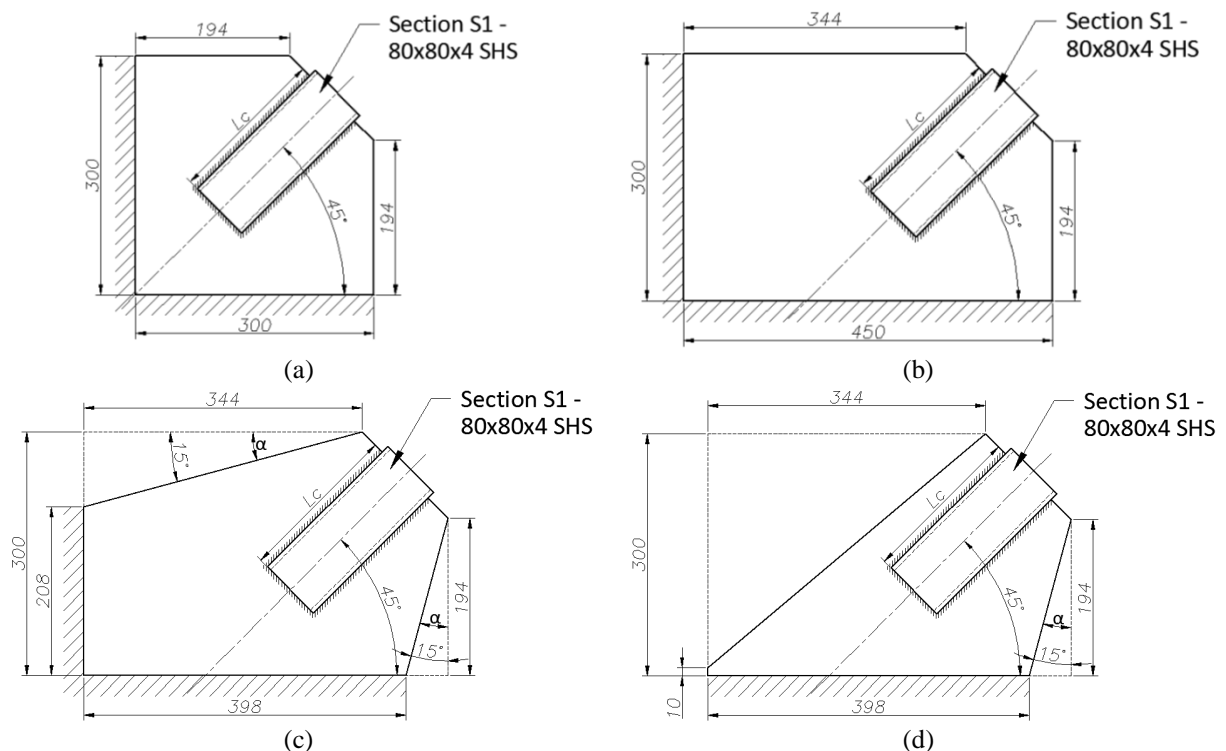
Figure 4.1. (a)-(d): Selected study specimens taken from full range of 12 (a) GP04, (b) GP05, (c) GP09, (d) GP11

In all of the specimens considered in this study, the gusset plate is assumed to be welded to the beam and column or to the beam only as the case may be. An assumption in the FE model is that the weld has sufficient strength so that failure of the system will be in the brace or the gusset plate. This is a

reasonable assumption as the welds should be capable of reaching the plastic capacity of the gusset plate (Lehman *et al.* 2008). However, it can be quite difficult to calculate the plastic capacity of the gusset plate under current codified methods (CEN 2004). Codified approaches, such as Eurocode 8 (CEN 2004), typically specify that non-dissipative elements, such as welds, are determined by the yield capacity of the dissipative element, such as the brace, factored by an over-strength factor that accounts for the actual material strength and size of brace member chosen.

4.1. Monotonic Simulations

In order to calculate the yield capacity of the gusset plate, monotonic tensile simulations were completed. From the force-strain plots, the yield force was calculated using the 0.2% proof strength method. Then the effective area of the gusset plate was calculated based on the 0.2% yield force divided by the expected yield stress of the material. This area was then compared to the newly defined elliptical area, A_E, as in Equation 4.1.

$$A_E = t_p * b_E, \qquad \text{where} \tag{4.1}$$

$$b_E = \beta_i * b \tag{4.2}$$

where, t_p is the plate thickness, b is the total width of the elliptical curve based on the $8t_p$ method as described by Lehman *et al.* (2008) and b_E is the effective width of the elliptical curve, as shown in Figure 4.2. This effective width is calculated by including a modification factor, β_i to account for the fact that not all of the plate is fully utilised in resisting the demand from the brace. This β-value is defined as the ratio of the calculated width (obtained from the numerical analysis) to the actual measured width of the elliptical curve and was calculated for all specimens in the study. The β-values are grouped into three distinct classes, namely, β_1 for rectangular plates connected to both beam and column, β_2 for tapered plates connected to both beam and column, and β_3 for plates connected to the beam only. The expressions developed for each of these are given in Equation 4.3, where α is the angle of the taper as indicated in Figure 4.1. The value obtained for β_1 was taken as the average value for all of the rectangular plates connected to the beam and column. The average value for all the tapered plates was also calculated and showed good agreement to the proposed formulae for β_2.

$$\beta_1 = 0.67; \quad \beta_2 = \beta_1 + 2tan\alpha(1 - \beta_1) \leq 1.0; \quad \beta_3 = 1.0; \tag{4.3}$$

This proposed method for calculating the effective area is an alternative procedure over the commonly used effective width or Whitmore width method (Whitmore 1952). Comparison of the gusset yield strengths ($N_{pl,Rd}$) calculated using both the Whitmore width and the proposed elliptical width to those estimated from numerical models are shown in Table 4.1. The system ID used in this table is referenced as follows: *GP05-6* references gusset plate 05 with a thickness t_p of 6mm. The brace connection length, L_c, was determined using the procedure outlined by Lehman *et al.* (2008).
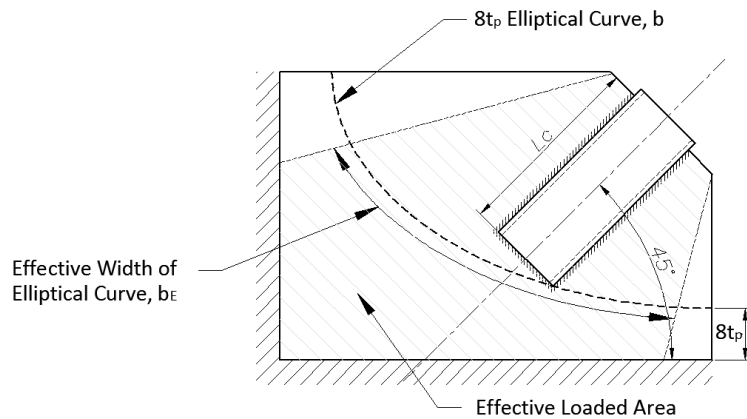
Figure 4.2. Gusset plate highlighting the effective loaded zone

As seen from Table 4.1, quite a good agreement exists between the proposed new elliptical width method and the numerical model for varies plate configurations. On the other hand, the Whitmore method under-estimates the effective width and, hence, under-estimates the yield capacity of the gusset plate by between 5 and 20%, which could have significant consequences for the performance of CBFs during earthquakes.

Table 4.1. Comparison of gusset yield strengths ($N_{pl,Rd}$) estimated from numerical models to those using the proposed elliptical width method and Whitmore width method

System	t_p	L_c	$N_{pl, Rd}$			(1) / (2)	(1) / (3)
			Numerical model (1)	New elliptical width method (2)	Whitmore method (3)		
ID	*(mm)*	*(mm)*	*(kN)*	*(kN)*	*(kN)*		
GP05-3	3	234	521	517	405	0.99	0.78
GP05-6	6	207	953	954	829	1.00	0.87
GP09-3	3	209	476	461	407	0.97	0.86
GP09-6	6	184	877	847	829	0.97	0.95
GP11-3	3	213	383	357	321	0.93	0.84
GP11-6	6	187	717	661	667	0.92	0.93

4.2. Cyclic Simulations

Normalised slenderness of the brace member has been shown not only to influence its buckling capacity, but also its ductility and energy dissipation capabilities (Goggins *et al* 2005). Eurocode 8 (CEN 2004) specifies limits for the normalised slenderness of brace members in CBFs. For X-braced systems, the normalised slenderness should be limited to $1.3 \leq \bar{\lambda} \leq 2.0$ and less than or equal to 2.0 for CBFs other than X-brace frames. What is of considerable interest is that the normalised slenderness of the brace is normally calculated without considering the effect of the gusset plate. It is important to stress that the gusset plate can have a significant effect on the normalised slenderness of the system. According to Eurocode 3 (CEN 2005), the effective length of the diagonal brace can be assumed to be pinned at both ends for the calculation of the normalised slenderness. Depending on the relative properties of the gusset plate and brace member, this assumption may not be valid.

It is for this reason that the gusset-brace as a system was studied and compared to an equivalent brace-only system, as shown in Figure 4.3. When considering the brace member independently of the gusset plate, two extremes of fixity were considered – pinned and fully fixed. The two approaches give a range of possible normalised slenderness in the actual system ($\bar{\lambda}_{pin}$ to $\bar{\lambda}_{fix}$), where the interaction of the gusset plate and brace is a complicated one. The buckling mode of the system is dependent on the relative slenderness of the gusset plate and brace member. If the relative slenderness of the brace is greater than that of the gusset, global brace buckling will be dominant and favourable. If the opposite is true, then gusset buckling will first dominate and this may potentially limit the ductility and energy dissipation of the system.

With reference to Table 4.2 the dimensions of the brace specimens used in this study can be seen, where S1L, I and S denote an 80x80x4 hollow brace section of lengths (L_{equiv}) 6, 4 and 2m respectively. Their yield displacements (δ_{equiv}) and normalised slendernesses assuming pinned and fully fixed end connections ($\bar{\lambda}_{pin}$ and $\bar{\lambda}_{fix}$, respectively) are also given in Table 4.2. All steel in this study is hot rolled carbon steel of grade S355.
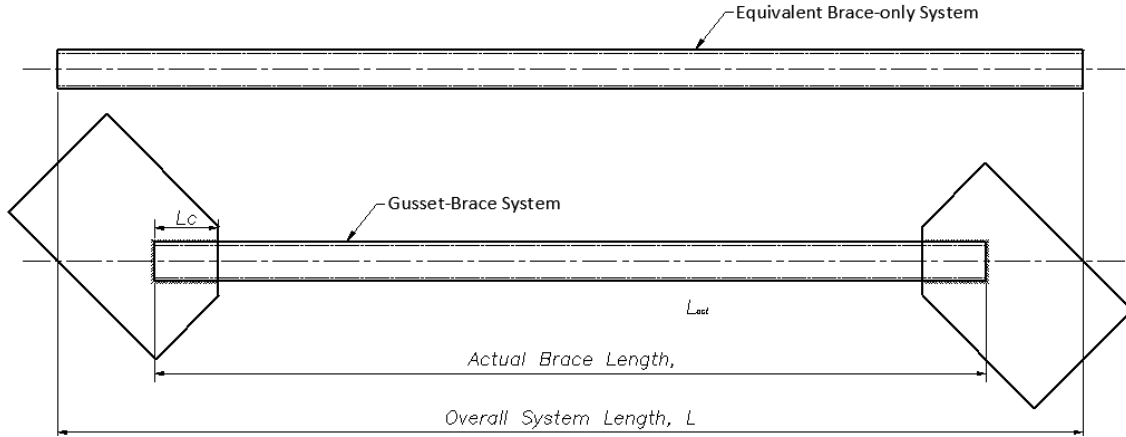
Figure 4.3. Comparison of gusset-brace system to equivalent brace-only system

Table 4.2. Properties of the brace sections used throughout this study.

System ID	Section ID	L_{equiv} (mm)	$\delta_{y, equiv}$ (mm)	$N_{pl,.Rd}$ (kN)	$\bar{\lambda}_{pin}$	$\bar{\lambda}_{fix}$
S1L	S1	6000	12.92	558	2.92	1.46
S1I	S1	4000	8.61	558	1.94	0.97
S1S	S1	2000	4.31	558	0.97	0.49

Considering the results of the study, as shown in Table 4.3, the gusset plate plays a significant role in the behaviour of the system. The first three rows in the table are the results of the brace-only system, which are used as the point of reference for all other gusset-brace results and are modelled as fixed ended specimens. The degree of fixity of the remaining study specimens (*GP04*, *05*, *09* and *11*), depend on the gusset plate geometry, and would be classed as having partial fixity. Shown in Table 4.3 are the tensile yield capacities of the gusset plate, $N_{pl,Rd, gusset}$, as detailed in Section 4.1, the critical buckling load and the normalised slenderness of the gusset-brace system, $F_{cr, sys}$ and $\bar{\lambda}_{sys}$ respectively, the number of cycles until fracture, N_f, and the corresponding ductility, μ_Δ of the system. The hysteretic energy, W_i at the eight, tenth and twelfth cycle are also shown normalised by the area under a yield load-displacement plot of the brace specimen, W_y.

The normalised slenderness of the system, $\bar{\lambda}_{sys}$, is calculated assuming brace-only equivalent properties, as the brace is still the primary dissipating member of the system, as in Equation 4.4. Referring to Figure 4.4a, the buckling curve for a hollow section member (buckling curve a, EC3 (CEN 2005)) is plotted along with the normalised slenderness of the gusset-brace system. It can be observed that for normalised slenderness values above 2.0, the gusset-brace system converges to that of a brace only system as the brace slenderness is dominant. For values below 2.0, the gusset-brace system has an enhanced buckling capacity over the brace-only system, as the gusset plate takes on a more dominant role in the system.

$$\bar{\lambda}_{sys} = \sqrt{\frac{f_{y,brace} * A_{brace}}{F_{cr,FE}}}; \qquad or \qquad \bar{\lambda}_{sys} = \sqrt{\frac{N_{pl,Rd\ brace}}{F_{cr,FE}}} \qquad (4.4)$$

As noted in Table 4.3, the primary failure mode for all specimens expect one was brace fracture at mid-length. Specimen *GP11-10-S1S* was the only case that exhibited extreme gusset plate buckling leading to fracture due to the combination of low brace slenderness and reduced gusset fixity, which was to the beam only. Hence, failure was due to fracture of the gusset plate in the area surrounding the end of the brace member. All specimens exhibited a ductility capacity, μ_Δ, of at least 4 with some of the more slender members achieving a ductility capacity of 6, as shown in Table 4.3. As expected, the energy dissipation by the system normalised to the elastic energy, W_y, in general, decreases with

increase in slenderness, as highlighted in Table 4.3 and Figure 4.4b. The energy index, plotted in Figure 4b, is defined as the area under the hysteretic curve up to the 1st cycle at a ductility of 4 and normalised by the elastic energy of the brace member. Comparisons are made to an expression derived for the energy index by Goggins *et al.* (2005), which underestimates the energy index of the gusset-brace systems. This may be due to the energy dissipation capabilities of the gusset plates in the current study, whereas the physical tests carried out by Goggins *et al.* (2005) on which the energy index expression is based had rigid connections with no gusset plates.

5. CONCLUSIONS

This study focuses on the relative properties of the gusset-brace as a system and highlights the effects that differing gusset plate geometries and configurations have on the system as a whole. Nearly all of the gusset plate systems included in this study were designed using the 8t$_p$ elliptical method. It was shown that the Whitmore width method overestimates the yield tensile capacity of the gusset plate and a new method to estimate an effective width based on the 8t$_p$ elliptical method was proposed. This method allows for improved ductility and energy dissipation of the system when compared to conventional gusset plate design. It was shown that the gusset-brace system tends to behave more like a fixed ended brace-only system the stockier the gusset plates become. This is the effect that conventional gusset plate design has on a CBF and this study highlights the benefits in paying more attention to gusset plate details to improve overall system performance.

Table 4.3. Results of the parametric study

System ID	Gusset Plate Properties				FE Results						
	t_p	L_c	b_E	$N_{pl,Rd, gusset}$	$F_{cr\ sys}$	$\bar{\lambda}_{sys}$	N_f	μ_Δ	W_8/W_y	W_{10}/W_y	W_{12}/W_y
	(mm)	*(mm)*	*(mm)*	*(kN)*	*(kN)*						
S1L	-	-	-	-	238[1]	1.53	11	6	10.2	15.4	16.4
S1I	-	-	-	-	410[1]	1.17	9	4	12.2	17.7	19.3
S1S	-	-	-	-	452[1]	1.11	10	4	17.6	24.8	27.8
GP04-6-S1I	6	174	258	720	176[1]	1.78	10	4	9.4	14.2	14.8
GP04-10-S1I	10	141	219	1018	198[1]	1.68	10	4	9.9	14.8	15.6
GP05-10-S1L	10	170	305	1418	96[1]	2.41	12	6	7.9	12.8	13.2
GP05-16-S1L	16	114	249	1853	123[1]	2.13	9	4	8.2	12.6	12.8
GP05-10-S1I	10	170	305	1418	187[1]	1.73	10	4	9.5	14.3	15.0
GP05-16-S1I	16	114	249	1853	236[1]	1.54	9	4	9.8	14.4	15.0
GP05-10-S1S	10	170	305	1418	412[1]	1.16	8	4	13.2	19.0	20.8
GP05-16-S1S	16	114	249	1853	448[1]	1.12	8	4	13.8	19.5	21.7
GP09-16-S1L	16	98	211	1570	112[1]	2.23	11	6	7.9	12.4	12.6
GP09-24-S1L*	24	98*	211	2355	164[1]	1.85	10	4	8.7	13.2	13.9
GP09-10-S1I	10	150	264	1228	179[1]	1.77	10	4	9.2	13.9	14.3
GP09-16-S1I	16	98	211	1570	223[1]	1.58	9	4	9.4	13.9	14.3
GP09-24-S1I*	24	98*	211	2355	305[1]	1.35	8	4	11.2	16.3	17.5
GP11-10-S1I	10	152	210	977	172[1]	1.80	11	6	9.3	13.9	14.2
GP11-16-S1I	16	100	170	1265	183[1]	1.75	11	6	9.0	13.7	14.1
GP11-10-S1S	10	152	210	977	390[2]	1.20	9	4	11.3	17.3	19.6

NOTE: * indicates that the 8t$_p$ method was <u>NOT</u> used, [1] indicates fracture at mid-span of the brace and [2] indicates fracture of the gusset plate
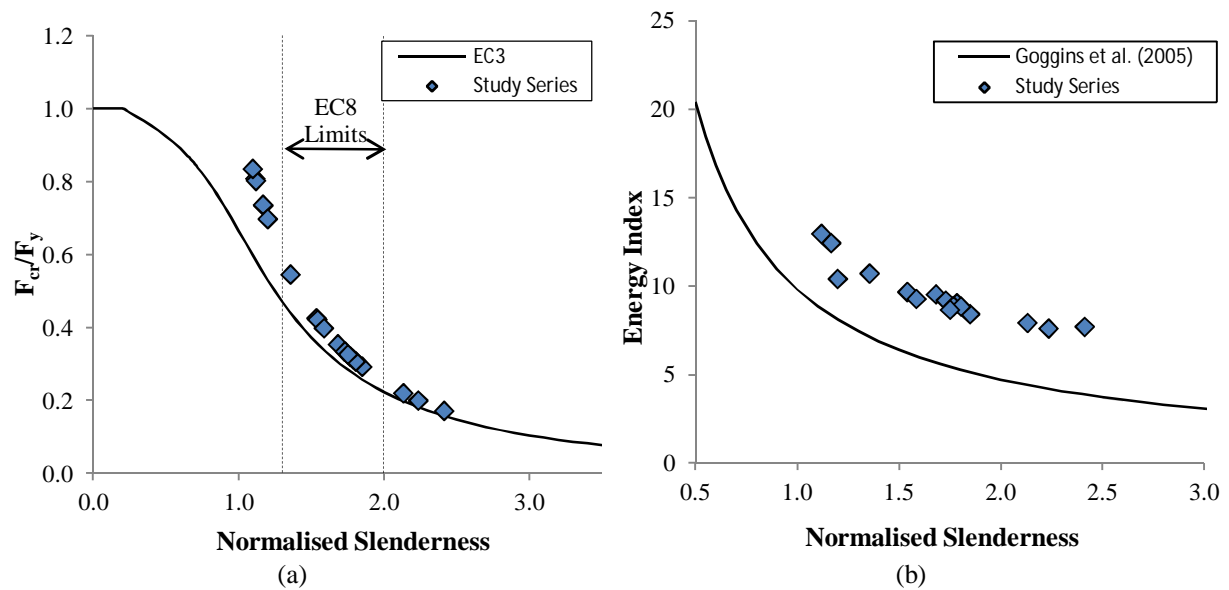
Figure 4.4. Normalised system slenderness versus (a) normalised critical load and (b) normalised hysteretic energy (energy index)

REFERENCES

ABAQUS (2009). Analysis User's Manual I-V. Version 6.9 USA. I. ABAQUS, Dassault Systems.

CEN (2004). Eurocode 8: Design of structures for earthquake resistance - Part 1: General rules, seismic actions and rules for buildings. European Standard, CEN (2004). ENV 1998-1:2004.

CEN (2005). Eurocode 3: Design of steel structures - Part 1-1: General rules and rules for buildings. ENV 1993-1-1:2005.

Broderick B, Hunt A, Goggins J, Elghazouli AY, LeMaoult A, Beg D, Queval J, Plumier A (2011) "Concentrically Braced Frame Model for Seismic Testing", *Eurosteel 2011,* **ECCS European Convention for Constructional Steelwork, 2011**, Pages:1137-1142

Goggins, J. M. (2004). Earthquake resistant hollow and filled steel braces, Trinity College, University of Dublin. *PhD Thesis.*

Goggins, J. M., Broderick, B. M., Elghazouli, A. Y. and Lucas, A. S. (2005). "Experimental cyclic response of cold-formed hollow steel bracing members." *Engineering Structures* **27(7):** 977-989.

Lehman, D. E., Roeder, C. W., Herman, D., Johnson, S. and Kotulka, B. (2008). "Improved Seismic Performance of Gusset Plate Connections." *Journal of Structural Engineering* **134(6):** 890-901.

Nascimbene, R., Rassati, G. A. and Wijesundara, K. K. (2012). "Numerical simulation of gusset plate connections with rectangular hollow section shape brace under quasi-static cyclic loading." *Journal of Constructional Steel Research* **70(0):** 177-189.

Nip, K. H., Gardner, L., Davies, C. M. and Elghazouli, A. Y. (2010b). "Extremely low cycle fatigue tests on structural carbon steel and stainless steel." *Journal of Constructional Steel Research* **66(1):** 96-110.

Nip, K. H., Gardner, L. and Elghazouli, A. Y. (2010a). "Cyclic testing and numerical modelling of carbon steel and stainless steel tubular bracing members." *Engineering Structures* **32(2):** 424-441.

Stoakes, C. D. and Fahnestock, L. A. (2012). "Cyclic flexural analysis and behavior of beam-column connections with gusset plates." *Journal of Constructional Steel Research* **72(0):** 227-239.

Whitmore, R. E. (1952). Experimental investigation of stresses in gusset plates, University of Tennessee, Knoxville, Tennessee.

Yoo, J.-H., Roeder, C. W. and Lehman, D. E. (2009). "Simulated behavior of multi-story X-braced frames."

  Engineering Structures **31(1):** 182-197.